ORIGINAL ARTICLE

Core/shell-like structured ultrafine branched nanofibers created by electrospinning

Makoto Konno, Yuuko Kishi, Manabu Tanaka and Hiroyoshi Kawakami

The fabrication of core/shell structured ultrafine nanofibers is an important challenge in nanomaterials because of their many potential future applications. We succeeded in fabricating novel core/shell-like nanofibers by a phase-separation process during the electrospinning of simple blend solutions containing various ratios of polyacrylonitrile (PAN) and fluorinated polyimide (PI). In addition, it was revealed that certain blend ratios produced branch structured nanofibers while maintaining the core/shell-like structures. Selective extraction of PI by acetone immersion and characterization by scanning electron microscope, Fourier transform infrared and X-ray photoelectron spectroscopy clearly demonstrated that the shell layer and the branched moieties were composed of PI, whereas the core domain was mainly formed by PAN. The process enabled control over the thicknesses of the core and shell domains as well as the diameter of the branched moieties derived from the main nanofibers by changing the molecular weight of PI. Interestingly, the water contact angle of nanofibrous membranes composed of PI/PAN = 80/20 (wt/wt) was 144°, indicating strong hydrophobicity of the nanofibers. These results demonstrated that the core/shell structured branched nanofibers can control the surface properties and have greater potential for the development of highly functional nanomaterials.

INTRODUCTION

Nanomaterials possess many unique chemical, mechanical, electrical and other properties, which are expected to result in revolutionary new materials and devices. There have been many reports on nanomaterials, such as nanoparticles, carbon nanotubes, molecular self-assembled materials and various nanocomposites.[1–4] However, these nanomaterials have been produced mostly by synthetic bottom-up methods and were discontinuous objects in many cases, leading to difficulties in their assembly, alignment and processing for actual applications. In contrast, electrospinning is easily capable of producing continuous fibers with diameters in the nanometer range.[5] A wide variety of electrospun nanofibers have been successfully prepared for many applications, including filters,[6] flexible electrodes,[7,8] optical and chemical sensors,[9] electrochemical devices,[10,11] catalyst systems[12] and scaffolds for tissue regeneration.[13,14] The main advantage of this top-down technology is its relatively low cost compared with most bottom-up methods; electrospinning technology has been employed for the cost-effective manufacturing of two- or three-dimensional nanofiber assemblies.[15,16] However, controlling the structure of the nanofibers is quite difficult compared with nanomaterials prepared by bottom-up methods, and precise structural control over electrospun nanofibers is desired.

The preparation of core/shell structured ultrafine nanofibers is an important challenge in electrospinning, because core/shell nanofibers have attracted considerable attention for their many possible applications, which include conductive nanofibers coated with an insulator, sensing devices on a rigid scaffold and controlled release in a drug-delivery system. In the past, core/shell nanofibers have been prepared either by coaxial electrospinning using double-channel spinnerets[17,18] or by using a polymer blend system prepared in immiscible mixed solvents, referred to as emulsion electrospinning.[19,20] In particular, in the latter case, a third component has often been introduced to the blended system to modify the properties of the binary polymer blend or to induce the blended dispersions. However, the mechanism of core/shell nanofiber formation in polymer blend systems is very complicated, and controlling the properties of the nanofibers, such as the thicknesses of the core and shell layers, is difficult. Although several studies have reported the formation of core/shell nanofibers by electrospinning polymer blends in a single solvent,[21–24] the fabrication and structural control over the core/shell nanofibers from blend systems is still challenging. In addition, to the best of our knowledge, such core/shell nanofibers have only been prepared from limited combinations of blend polymers, including polyacrylonitrile (PAN) and poly(methyl methacrylate),[21,22] polyaniline and polystyrene,[23] or polybutadiene and polycarbonate.[24] Expanding the possible polymer blend combinations and achieving the formation of additional unique nanostructures would produce a major breakthrough in nanofibers and greatly impact the application of electrospinning.

In this study, we report core/shell-like nanofibers fabricated by electrospinning blend solutions of PAN and fluorinated polyimide (PI). PAN was selected because of its chemical properties and good

Department of Applied Chemistry, Tokyo Metropolitan University, Tokyo, Japan
Correspondence: Dr H Kawakami, Department of Applied Chemistry, Tokyo Metropolitan University, Minamiosawa, Hachioji, Tokyo 192-0397, Japan.
E-mail: kawakami-hiroyoshi@tmu.ac.jp

nanofiber forming ability, according to previous research.[21,22] However, PI was selected because of its good solubility in organic solvents and its successful use in preparing uniform, non-beaded polyimide nanofibers with diameters of approximately 40 nm.[25,26] PAN is an aliphatic polymer, and PI is an aromatic polymer. Thus their properties are quite different (Table 1). The influence of the PI/PAN blend ratio on nanofiber formation was carefully investigated to verify their core/shell nanostructures. Interestingly, it was revealed that certain blend ratios produced branch structured nanofibers while maintaining their core/shell-like structures. Selective extraction of PI by acetone immersion and characterization by scanning electron microscope (SEM), Fourier transform infrared (FT-IR) and X-ray photoelectron spectroscopy (XPS) clearly demonstrated that the shell layer and the branched moiety were composed of the PI, whereas the core domain was mainly formed by PAN. The mechanism behind the formation of the core/shell-like structured ultrafine branched nanofibers by electrospinning is also discussed. Furthermore, the nanofibrous membranes were demonstrated to have unique, strongly hydrophobic properties, which could make this nanomaterial useful for future applications.

EXPERIMENTAL PROCEDURE

Materials
2,2′-Bis(3,4-dicarboxyphenyl)hexafluoropropane dianhydride (6FDA) and 2,2′-bis(4-aminophenyl)hexafluoropropane (6FAP) were purchased from the Central Glass Co. (Saitama, Japan). 6FDA was purified by sublimation prior to use. 6FAP was recrystallized twice from an ethanol solution prior to use. PAN was purchased from the Aldrich Chemical Co. (Milwaukee, WI, USA) and was used without pretreatment. Other chemicals were obtained from the Kanto Chemical Co. (Tokyo, Japan) and were used as received.

Synthesis and characterization of 6FDA-6FAP
The PI 6FDA-6FAP was synthesized by chemical imidization of the poly(amic acid) precursors, as reported in the literature.[25–27] The structure of PI is shown in Table 1. The molecular weights (M_w and M_n) of PI were determined by gel permeation chromatography (detector: Jasco 830-RI monitor, JASCO, Tokyo, Japan) with tetrahydrofuranas the solvent. A flow rate of $1.0\,\mathrm{ml\,min^{-1}}$ was used, and the PI was dissolved in tetrahydrofuran at a concentration of 0.005 wt%. The molecular weights were estimated by comparing the retention times on the column (Shodex KF-805L, Showa Denko K.K., Tokyo, Japan) to those of polystyrene standards.

Preparation of nanofibers
The nanofibers were fabricated using an electrospinning apparatus (Fuence, Co., Ltd., ES-1000, Tokyo, Japan).[25,26] PI was dissolved in anhydrous dimethylformamide (DMF) at room temperature. PAN was dissolved in anhydrous DMF at 60 °C. These two solutions were mixed to obtain blend solutions with different blend ratios (PI/PAN = 100/0–0/100 (wt/wt)). The viscosities of the polymer solutions were measured using a rotational viscometer (RE-85, Toki Sangyo, Tokyo, Japan). In a typical electrospinning process, the polymer mixture solution with a 17 wt% concentration was loaded into a 1-ml syringe as the spinneret. Then a syringe pump was used to supply a steady flow of polymer solution at $0.12\,\mathrm{ml\,h^{-1}}$ through a needle with an inner diameter of 0.21 mm. A voltage of 10 kV was applied between the syringe and the collector. The distance between the syringe spinneret and the grounded collector plate was 10 cm. The humidity in the electrospinning apparatus was $5 \pm 2\%$RH (relative humidity). The nanofibrous membranes were deposited onto an aluminum sheet by electrospinning. To remove residual solvent from the fabricated nanofibers, the samples were vacuum dried at 70 °C for 10 h.
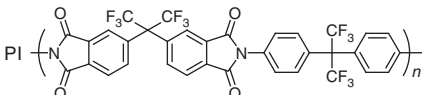
Characterization
The glass transition temperatures (T_g) of PI and PAN were measured using a differential scanning calorimeter (DSC, DSC-60, Shimadzu, Kyoto, Japan). The morphological characteristics of the nanofibrous membranes, such as the diameter of the nanofibers, were evaluated using a SEM (JXP-6100P, JEOL, Tokyo, Japan). At least 25 pictures were used to calculate the average diameter of the nanofibers for each formulation. XPS (ESCA3400, Shimadzu) was carried out using a monochromatic MgKα X-ray source (1253.6 eV photons) to measure the elemental ratios in the nanofibers and monitor chemical changes on the nanofiber surfaces. The surface changes in the PI/PAN nanofibers were investigated by FT-IR spectroscopy combined with attenuated total reflectance (FT-IR-ATR 6100 V, JASCO). The water contact angles (WCA) of PI/PAN cast membranes and nanofibrous membranes were measured using an Erma Contact Angler meter (Goniometer, Type.G-1, Erma Co., Krüss, Germany). At least 10 samples were measured per membrane composition, and the WCA was determined by averaging the results. The polymer–solvent (DMF) interaction parameters (χ) were calculated based on the Flory–Huggins solution theory and the intrinsic viscosities of the polymers.[28] The intrinsic viscosities of the polymers were measured with an Ostwald viscometer (SIBATA Scientific Technology Ltd., Saitama, Japan).
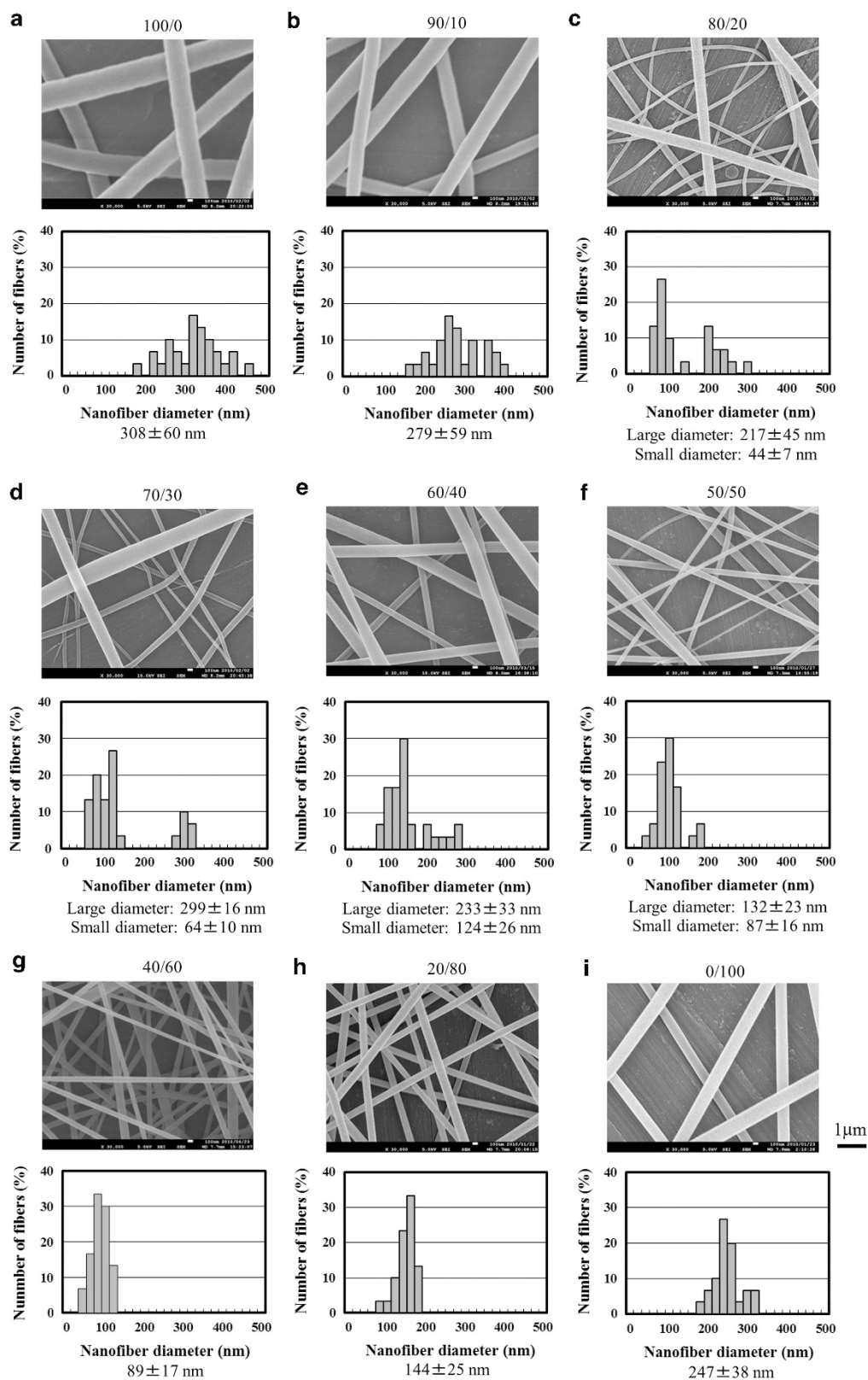
RESULTS AND DISCUSSION

Preparation of electrospun nanofibers
The soluble aromatic polyimide containing CF_3 groups, PI, was synthesized by chemical imidization involving treatment with a mixture of acetic anhydride and triethylamine to produce a high molecular weight ($M_w = 3.2 \times 10^5$) and a narrow polydispersity index ($M_w/M_n = 2.0$). The molecular weight of PAN was 1.5×10^5. In this study, 17 wt% DMF solutions of polymers with various PI/PAN blend ratios were prepared and used to fabricate continuous non-beaded nanofibers. The morphologies, diameter distributions and average diameters of the nanofibers prepared from various PI/PAN blend ratios are shown in Figure 1. The average diameters of the nanofibers

---

Table 1 Chemical structures and characteristics of the fluorinated polyimide (PI) and polyacrylonitrile (PAN)

Chemical structure	M_w	T_g	WCA	χ_{23} (DMF)
PI	3.2×10^5	360	100	0.439
PAN	1.5×10^5	85	60	0.343

Abbreviations: DMF, dimethylformamide; M_w, molecular weight; T_g, glass transition temperature (°C); WCA, water contact angle (degree); χ_{23}, polymer–solvent interaction parameter.
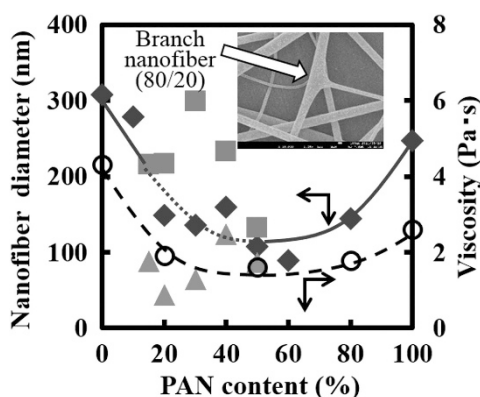
a 100/0

308±60 nm

b 90/10

279±59 nm

c 80/20

Large diameter: 217±45 nm
Small diameter: 44±7 nm

d 70/30

Large diameter: 299±16 nm
Small diameter: 64±10 nm

e 60/40

Large diameter: 233±33 nm
Small diameter: 124±26 nm

f 50/50

Large diameter: 132±23 nm
Small diameter: 87±16 nm

g 40/60

89±17 nm

h 20/80

144±25 nm

i 0/100

247±38 nm

Figure 1 SEM images and nanofiber diameter distributions of the blended nanofibers. PI/PAN ratios of (**a**) 100/0, (**b**) 90/10, (**c**) 80/20, (**d**) 70/30, (**e**) 60/40, (**f**) 50/50, (**g**) 40/60, (**h**) 20/80 and (**i**) 0/100. A full color version of this figure is available at *Polymer Journal* online.

prepared from the polymer blend (PI/PAN) were smaller than those of pure PI or pure PAN nanofibers because of the low solution viscosity, which enabled the polymer chains to be easily stretched during the electrospinning process, thereby producing thinner nanofibers. In addition, the nanofibers prepared from blend ratios (PI/PAN) in the range of 50/50–80/20 had two markedly different diameters, as shown in the distributions of nanofiber diameters. The relationship between nanofiber diameter and PAN content in the blended nanofibers is summarized in Figure 2. There is a good correlation between the average diameter of the nanofibers and the viscosity of the polymer solution used for electrospinning. Polymer concentration and the viscosity of a polymer solution are two of the most important parameters that influence the diameter of electrospun nanofibers. In general, the diameter of a non-beaded nanofiber prepared by electrospinning gradually decreases with decreasing polymer concentration.[25] The average diameters of the blended nanofibers also decreased with decreasing viscosity of the polymer solution (Figure 2). The low viscosities in the PI/PAN blend solutions may have been derived from the immiscibility of hydrophobic PI and

hydrophilic PAN, which would induce phase separation during the electrospinning process.

As shown in the representative SEM images in Figure 2, the nanofibers in the 50/50–80/20 blend ratios (PI/PAN) showed the formation of branched structures. The two markedly different nanofiber diameters for the PI/PAN blend ratios in this range resulted from the formation of these branched structures. The branching formation ratio, which was calculated from the number of branch points divided by the total number of main nanofibers, in the blended nanofibers was plotted as a function of the PAN content in Figure 3a. The branching formation ratio in the blended nanofibers increased with increasing applied voltage (Figure 3b). In general, similar branch formation has been observed for various single polymers from more concentrated and viscous solutions at a high applied voltage.[29] In addition, it has been shown that many branched nanofibers were formed when the diameter of the jet was relatively large, resulting in final diameters that were micrometers in size.[29,30] In contrast, the main nanofiber of the branched nanofibers prepared in this study presented a uniform, non-beaded morphology with a diameter <300 nm. In addition, the diameter of the branched moieties derived from the main nanofibers was also <100 nm.
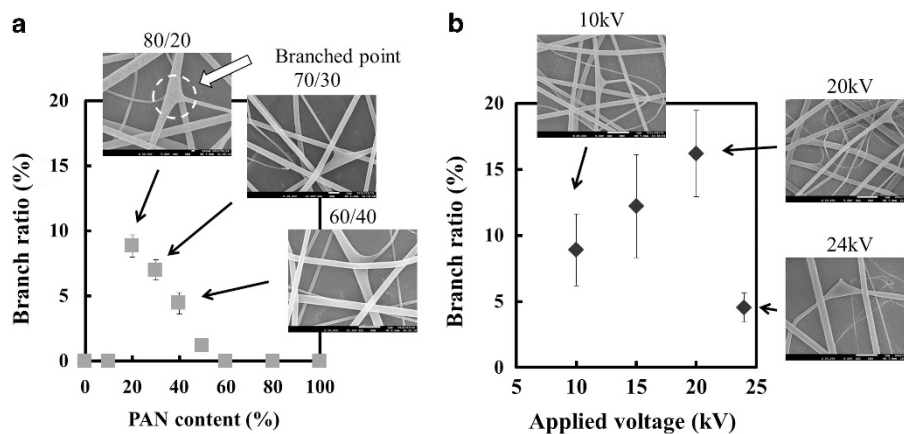
Characterization of the nanofibers

Hydrophobic and hydrophilic polymers may be segregated to the outside air surface and the inside of the polymer solution, respectively, during electrospinning. Therefore, we hypothesized that a PI layer, having stronger hydrophobicity, would be formed on the outside of the nanofibers, and PAN would be formed within the nanofibers as the core domain. This type of core/shell structure for the blended nanofibers could easily be confirmed using acetone, which is a good solvent for PI. Thus the selective extraction of PI from the branched nanofiber occurs by immersion in acetone. Surprisingly, the branched moieties completely disappeared after 1 h of immersion in acetone (Figure 4), indicating that the branched moieties were composed of PI. In addition, the main nanofibers became wrinkled and their diameter was slightly reduced from 217 to 207 nm. The nanofiber structures still remained.

The core/shell-like structure of the blended nanofibers (PI/PAN = 80/20) was further investigated based on the ATR FT-IR spectra of the nanofibers before and after immersion in acetone

Figure 2 Average diameters and solution viscosities for the blended nanofibers as a function of PAN content. ◆: the blended nanofibers, ■ and ▲: large and small diameters of the branched nanofibers, respectively, in the 50/50–80/20 range of blend ratios (PI/PAN), ○: viscosity of PI/PAN blend solutions. Inset: An SEM image of branched nanofibers (PI/PAN = 80/20). A full color version of this figure is available at *Polymer Journal* online.

Figure 3 SEM images and branch ratios of the blended nanofibers prepared from (**a**) different PI/PAN ratios at an applied voltage of 20 kV and (**b**) at different applied voltages (10, 15, 20 and 24 kV) and PI/PAN = 80/20. Branching formation ratio = (number of branched points)/(total number of main nanofibers). A full color version of this figure is available at *Polymer Journal* online.
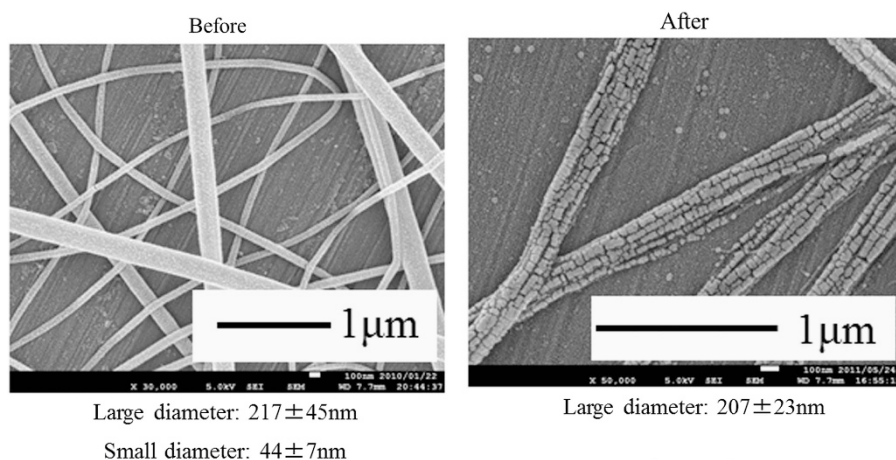
Before

After

Large diameter: 217±45nm

Small diameter: 44±7nm

Large diameter: 207±23nm

Figure 4 SEM images of the blended nanofibers (PI/PAN = 80/20) before and after immersion in acetone.
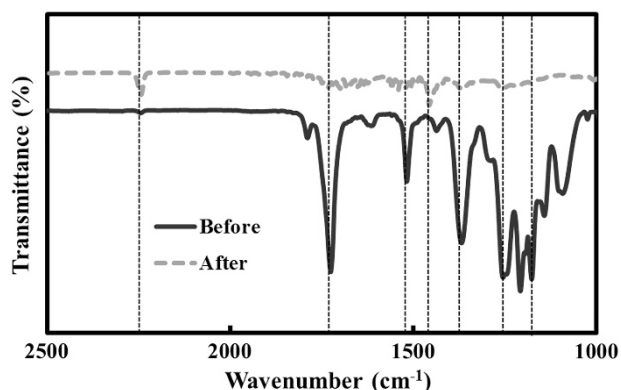

Figure 5 FT-IR spectra of the blended nanofibers (PI/PAN = 80/20) before (solid line) and after (dashed line) immersion in acetone. A full color version of this figure is available at *Polymer Journal* online.
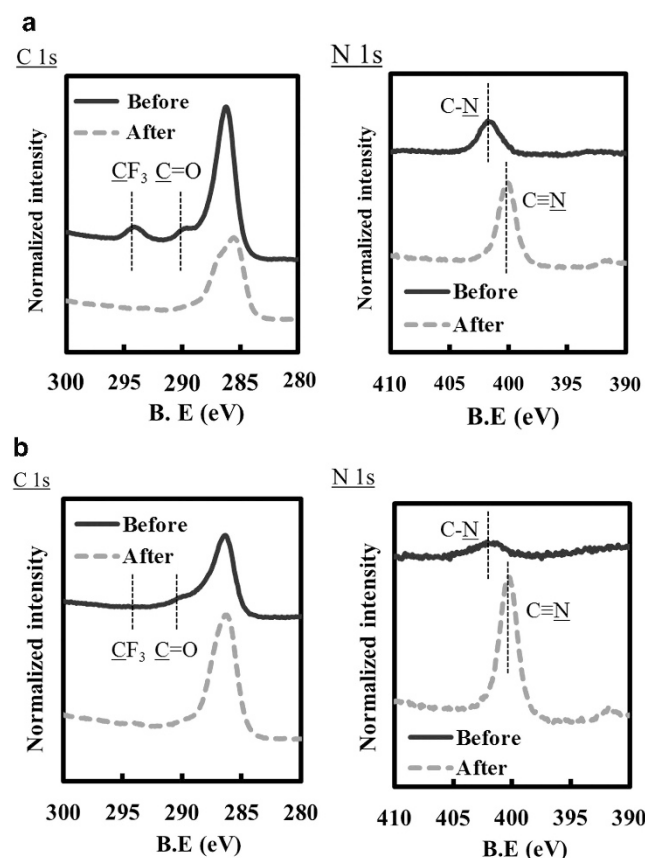

Figure 6 XPS spectra of the blended nanofibers of (**a**) PI/PAN = 80/20 and (**b**) PI/PAN = 20/80 before (solid line) and after (dashed line) immersion in acetone. A full color version of this figure is available at *Polymer Journal* online.

(Figure 5). There was a significant difference in the absorbance spectra before and after the immersion. Before the immersion, the spectra showed only the PI absorbance of the carbonyl (1725 cm^{-1}), CF$_3$ (1176–1255 cm^{-1}), imide (1368 cm^{-1}) and aromatic (1517 cm^{-1}) groups, indicating that PI existed on the outside of the nanofibers. However, after the immersion, these peaks completely disappeared, and new peaks appeared at approximately 1455 and 2244 cm^{-1}. These peaks correspond to the CH$_2$ and C≡N bands of PAN, respectively, indicating that the surface of the blended nanofibers changed to PAN. XPS measurements were also conducted to characterize the core/shell structure of the blended nanofibers (80/20) (Figure 6a). Before the immersion, peaks were observed at 294.2, 290.0 and 401.8 eV, corresponding to the carbon of CF$_3$, the carbon of C=O and the nitrogen of C-N in PI, respectively. These peaks derived from PI surface completely disappeared after the immersion, and a new peak appeared at 400.1 eV. This peak corresponds to the nitrogen of C≡N in PAN, supporting that the surface of the blend nanofibers changed to PAN.

These findings from ATR FT-IR and XPS confirm that the nanofibers were composed of PI-rich and PAN-rich phases and exhibited a relatively uniform non-beaded PI (shell)/PAN (core) structure along the fiber axis. Furthermore, the outer diameter of the fibers was approximately 200 nm with a wall thickness of approximately 5 nm (based on the reduction in the nanofiber diameter after

acetone immersion), indicating that the main nanofibers were coated by a thin PI layer, and most of the PI was utilized in the branch moieties in the branched nanofibers. The blended nanofibers with an inverted blend ratio (PI/PAN = 20/80) were also investigated by XPS spectroscopy before and after immersion in acetone (Figure 6b). After the immersion, the peaks on the polyimide surface completely disappeared and a new peak corresponding to PAN was observed,

indicating that these blended nanofibers (20/80) were also composed of PAN-rich core and PI-rich shell phases.

Formation mechanism for core/shell-like structured ultrafine branched nanofibers

Here we discuss the mechanism behind the formation of core/shell-like structured ultrafine branched nanofibers. It is known that most solutions containing several types of polymers induce immiscible blends because of their low mixing entropy. Thus, naturally, the electrospinning solution prepared from the polymer blend phase separates during the electrospinning process. We focused on the solvent (DMF)–polymer interaction parameter (χ) for both polymers (Table 1), because the ultra-rapid solvent evaporation that occurs during electrospinning is considered to be one of the key factors influencing the miscibility of a polymer blend. It is well known that a high χ indicates low compatibility of the solvent–polymer, while a low χ indicates a solvent and polymer with high mutual affinity.[28] Therefore we consider that differences in the affinity of PAN and PI for DMF induce instantaneous phase separation during the electrospinning process. In addition, the hydrophobic and hydrophilic polymers can be separated to the outside air-contacting surface and the inside of the polymer solution, respectively, when electrospinning is carried out for a blended polymer having both hydrophobic and hydrophilic domains under low relative humidity conditions ($5 \pm 2\%$RH). Consequently, because of its stronger hydrophobicity, the PI layer was formed on the outside of the nanofibers and PAN was formed within the nanofibers as the core domain. Branching phenomena have previously been modelled in terms of undulations occurring on the surface of the jet, controlled by the balance between the electric and surface forces.[30] The voltage applied during electrospinning influences the balance between the electric and surface forces and is one of the key factors that determines branching formation. Branch formation requires enough energy to create the additional surface area, and instability of the surface results in branching at the jet surface. In this study, the PI in the shell phase formed branch structures to create additional surface area before the PI formed thick shell layers in the relatively high PI blend ratios (PI/PAN = 50/50–80/20).

Surface properties of the nanofibers

WCA measurements were conducted to elucidate the surface properties resulting from the core/shell-like structure of the blended nanofibrous membranes, which were compared with blended cast membranes.[31,32] The WCA of the blended membranes decreased linearly with increasing PAN content owing to the presence of the hydrophilic PAN (Figure 7). In contrast, the WCA of the PI nanofibrous membrane was 120°, which was much higher than that of the PI cast membrane. The increased WCA value compared with the cast membrane can be explained by the Cassie–Baxter model,[33] which takes into account the presence of air gaps between individual nanofibers that limit droplet penetration into a porous nanostructure compared with a membrane of the same material (Figure 8a). For the core/shell-like structured blended nanofibrous membrane (PI/PAN = 20/80), the WCA was similar to that of the PI nanofibrous membrane and was measured to be 120°, owing to the presence of a hydrophobic PI surface layer. These results strongly support the core/shell structure of the blended nanofibers. However, the WCA increased with a decreasing PAN content from 50/50 to 80/20 in the PI/PAN blend ratio and reached 144° at the 80/20 ratio, indicating the strong hydrophobicity of the blended nanofibrous membrane. Hydrophobicity can be significantly enhanced by increasing the
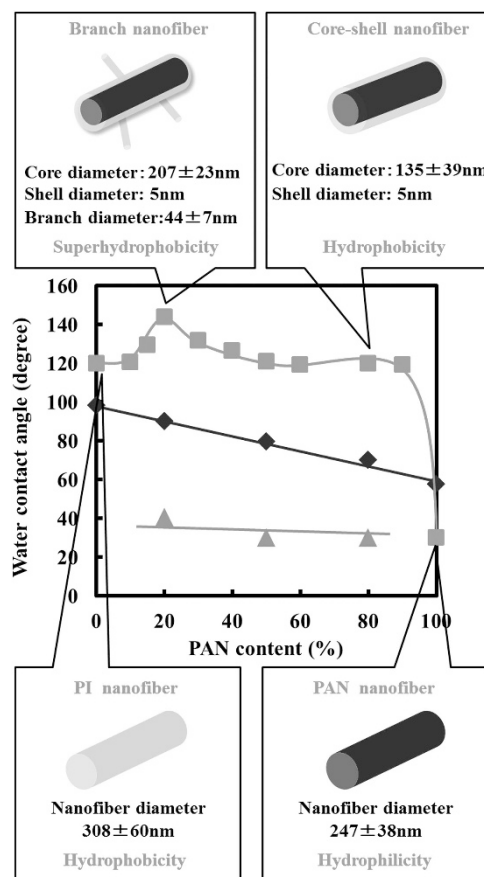

Figure 7 Water contact angles of blended nanofibrous membranes (■: before immersion in acetone, ▲: after immersion in acetone) and blended cast membranes (◆). Schematic illustrations and the core/shell domain sizes of the blended nanofibrous membranes before immersion in acetone are also shown. A full color version of this figure is available at *Polymer Journal* online.

surface roughness or lowering the surface energy.[33] However, the surfaces of the core/shell structured blended nanofibers were encapsulated by the PI layer. Furthermore, the surface energy should not be dependent on the blend ratio, but rather, should be constant. The diameter of the blended nanofibers was also anticipated to be an important factor influencing the hydrophobicity of the nanofibrous membranes. However, the WCAs of the PI and PAN nanofibrous membranes were not influenced by differences in the diameters and were constant (Figure 8b). Consequently, we concluded that the branching ratio in the blended nanofibers significantly influenced the hydrophobicity of the nanofiber membranes. The surface roughness of nanofibrous membranes formed by mixtures of large diameter main nanofibers and the small diameter branched moieties may have induced the strong hydrophobicity of the branched nanofibers. Recently, much attention has been paid to superhydrophobic nanofibrous membranes, because their formation is of great scientific and industrial importance for technical applications, such as water repellency, self-cleaning and antifouling properties.[34,35] In general, the core/shell structured nanofibers indicate a constant WCA value owing to the encapsulated polymer layer, and the value does not depend on the polymer blend ratio. In contrast, the core/shell-like structured branched nanofibers can control the surface properties and have greater potential for the discovery of highly functional nanomaterials.
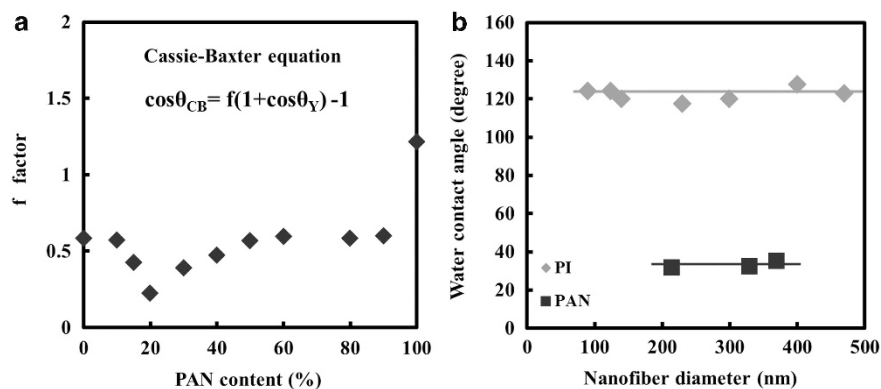
Figure 8 (**a**) Calculated *f* factor of the blended nanofibrous membranes prepared from different PI/PAN ratios. *f*: the fraction of the droplet that is actually in contact with the surface, θ_{CB}: the contact angle on a rough surface, θ_Y: the contact angle on a smooth surface. (**b**) Influence of the nanofiber diameter on the water contact angle. A full color version of this figure is available at *Polymer Journal* online.
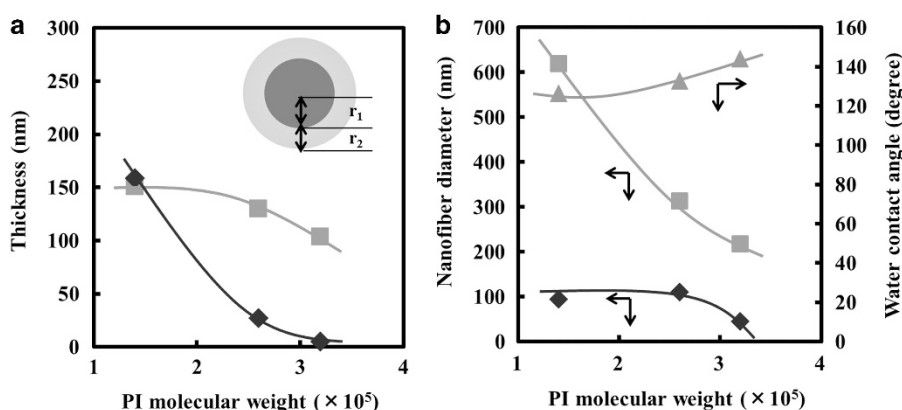
Figure 9 Effect of PI molecular weight on the characteristics of the PI/PAN = 80/20 blended nanofibers. (**a**) Core (r_1, ■) and shell (r_2, ◆) thicknesses of the blended nanofibers. (**b**) Diameters of the main nanofibers (■) and branched moieties derived from the main nanofiber (◆) of the branched nanofibers and water contact angles of the blended nanofibrous membranes (▲). A full color version of this figure is available at *Polymer Journal* online.

A better understanding of the relationship between the core/shell-like structured branched nanofibers and the diameter or WCA is of great importance for the development of novel core/shell nanofibers. It is well known that the nanofiber diameter is significantly affected by the molecular weight of the polymer.[25,26] Therefore, three types of PIs with different molecular weights, 1.4×10^5, 2.6×10^5 and 3.2×10^5, were used to prepare core/shell structured branched nanofibers with different diameters. The effects of the PI's molecular weight on the diameter and WCA of the core/shell-like structured branched nanofibers were investigated. As shown in Figure 9a, it is clear that the core and shell diameters of the branch nanofiber significantly decreased with increasing PI's molecular weight. The diameter of the branched moieties derived from the main nanofibers also decreased with increasing PI's molecular weight (Figure 9b). However, the WCA of the branched nanofibrous membranes increased with the molecular weight of PI because of the higher surface roughness of the branched nanofibers (PI: $M_w = 3.2 \times 10^5$) with narrower diameters compared with branched nanofibers (PI: $M_w = 1.5 \times 10^5$) with larger diameters.

In this study, PI with a WCA of 100° in the membrane state was utilized as a hydrophobic polymer. The selection of more hydrophobic polymer as one phase of the blend solution for electrospinning is expected to produce core/shell branched nanofibers bearing stronger hydrophobicity. These superhydrophobic core/shell branched nanofibers have the potential for not only self-cleaning and

antifouling applications but also for industrial applications, such as in nanocoatings, nanoreinforcement, nanocomposites, nanomedicine and drug-release systems.

CONCLUSIONS

Novel core/shell-like structured ultrafine branched nanofibers were successfully fabricated by a phase-separation process using simple polymer blend (PAN and PI) solutions with electrospinning. Specific PI/PAN blend ratios (from 50/50 to 80/20) provided core/shell-like branched nanofiber structures. In addition, we revealed that the PAN content and the applied voltage during the electrospinning process produced different branching ratios in the blended nanofibers. The core/shell-like structure was investigated by SEM, FT-IR and XPS analyses of the nanofibers before and after immersion in acetone, which selectively dissolved PI. The obtained core/shell-like structured branched nanofibrous membranes showed strong hydrophobicity, which was derived from the hydrophobic shell polymer and the ultrafine branched nanostructure. This simple process could be used to prepare core/shell structured branched nanofibers composed of other polymer blends and could also provide novel opportunities for industrial applications, such as in nanocoatings, nanoreinforcement, nanocomposites, nanomedicine and drug-release systems.

ACKNOWLEDGEMENTS

1   Baughman, R. H., Zakhidov, A. A. & de Heer, W. A. Carbon nanotubes–the route toward applications. *Science* **297**, 787–792 (2002).
2   Shimizu, T., Masuda, M. & Minamikawa, M. Supramolecular nanotube architectures based on amphiphilic molecules. *Chem. Rev.* **105**, 1401–1444 (2005).
3   Suzuki, M., Saruwatari, K., Kogure, T., Yamamoto, Y., Nishimura, T., Kato, T. & Nagasawa, H. An acidic matrix protein, Pif, is a key macromolecule for nacre formation. *Science* **325**, 1388–1390 (2009).
4   Bai, C. & Li, M. From chemistry to nanoscience: Not just a matter of size. *Angew. Chem. Int. Ed.* **52**, 2678–2683 (2013).
5   Dzenis, Y. Spinning continuous fibers for nanotechnology. *Science* **304**, 1917–1919 (2004).
6   Ma, H., Burger, C., Hsiao, B. S. & Chu, B. Ultrafine polysaccharide nanofibrous membranes for water purification. *Biomacromolecules* **12**, 970–976 (2011).
7   Sode, K., Sato, T., Tanaka, M., Suzuki, Y. & Kawakami, H. Carbon nanofibers prepared from electrospun polyimide, polysulfone and polyacrylonitrile nanofibers by ion-beam irradiation. *Polym. J.* **45**, 1210–1215 (2013).
8   Sode, K., Tanaka, M., Suzuki, Y. & Kawakami, H. Nickel nanoparticle chains inside carbonized polymer nanofibers: preparation by electrospinning and ion-beam irradiation. *Nanoscale* **5**, 8235–8241 (2013).
9   Wang, M., Meng, G., Huang, Q. & Qian, Y. Electrospun 1,4-DHAQ-doped cellulose nanofiber films for reusable fluorescence detection of trace Cu^{2+} and further for Cr^{3+}. *Environ. Sci. Technol.* **46**, 367–373 (2012).
10 Tamura, T. & Kawakami, H. Aligned electrospun nanofiber composite membranes for fuel cell electrolytes. *Nano Lett.* **10**, 1324–1328 (2010).
11 Imaizumi, S., Matsumoto, H., Ashizawa, M., Minagawa, M. & Tanioka, A. Nanosize effects of sulfonated carbon nanofiber fabrics for high capacity ion-exchanger. *RSC Advances* **2**, 3109–3114 (2012).
12 Arai, T., Tanaka, M. & Kawakami, H. Porphyrin-containing electrospun nanofibers: positional control of porphyrin molecules in nanofibers and their catalytic application. *ACS Appl. Mater. Interfaces* **4**, 5453–5457 (2012).
13 Holzwarth, J. M. & Ma, P. X. 3D nanofibrous scaffolds for tissue engineering. *J. Mater. Chem.* **21**, 10243–10251 (2011).
14 Jin, G., Prabhakaran, M. P., Kai, D., Kotaki, M. & Ramakrishna, S. Electrospun photosensitive nanofibers: potential for photocurrent therapy in skin regeneration. *Photochem. Photobiol. Sci.* **12**, 124–134 (2013).
15 Li, D. & Xia, Y. Electrospinning of nanofibers: Reinventing of wheel? *Adv. Mater.* **16**, 1151–1170 (2004).
16 Karube, Y. & Kawakami, H. Fabrication of well-aligned electrospun nanofibrous membrane based on fluorinated polyimide. *Polym. Adv. Technol.* **21**, 861–866 (2010).
17 Zhang, Y. Z., Wang, X., Feng, Y., Li, J., Lim, C. T. & Ramakrishna, S. Coaxial electrospinning of (fluorescein isothiocyanate-conjugated bovine serum albumin)-encapsulated poly(epsilon-caprolactone) nanofibers for sustained release. *Biomacromolecules* **7**, 1049–1057 (2006).
18 Pakravan, M., Heuzey, M. C. & Ajji, A. core-shell structured PEO-chitosan nanofibers by coaxial electrospinning. *Biomacromolecules* **13**, 412–421 (2012).
19 Xu, X., Zhuang, X., Chen, X., Wang, X., Yang, L. & Jing, X. Preparation of core-sheath composite nanofibers by emulsion electrospinning. *Macromol. Rapid Commun.* **27**, 1637–1642 (2006).
20 Choi, S. H., Youn, D. Y., Jo, S. M., Oh, S. G. & Kim, I. D. Micelle-mediated synthesis of single-crystalline β(3C)-SiC fibers via emulsion electrospinning. *ACS Appl. Mater. Interfaces* **3**, 1385–1389 (2011).
21 Bazilevsky, A. V. A., Yarin, A. L. & Megaridis, C. M. Co-electrospinning of core-shell fibers using a single-nozzle technique. *Langmuir* **23**, 2311–2314 (2007).
22 Zander, N. E., Strawhecker, K. E., Orlicki, J. A., Rawlett, A. M. & Beebe, T. P. Jr. Coaxial electrospun poly(methyl methacrylate)-polyacrylonitrile nanofibers: Atomic force microscopy and compositional characterization. *J. Phys. Chem. B* **115**, 12441–12447 (2011).
23 Wei, M., Lee, J., Kang, B. & Mead, J. Preparation of core-sheath nanofibers from conducting polymer blends. *Macromol. Rapid Commun.* **26**, 1127–1132 (2005).
24 Wei, M., Kang, B. W., Sung, C. M. & Mead, J. Core-sheath structure in electrospun nanofibers from polymer blends. *Macromol. Mater. Eng.* **291**, 1307–1314 (2006).
25 Fukushima, S., Karube, Y. & Kawakami, H. Preparation of ultrafine uniform electrospun polyimide nanofiber. *Polym. J.* **42**, 514–518 (2010).
26 Arai, T. & Kawakami, H. Ultrafine electrospun nanofiber created from cross-linked polyimide solution. *Polymer* **53**, 2217–2222 (2012).
27 Kawakami, H., Mikawa, M. & Nagaoka, S. Gas permeability and selectivity through asymmetric polyimide membranes. *J. Appl. Polym. Sci.* **62**, 965–971 (1996).
28 Kok, C. M. & Rudin, A. Prediction of Flory–Huggins interaction parameters from intrinsic viscosities. *J. Appl. Poly. Sci* **27**, 353–362 (1982).
29 Reneker, H. D. & Yarin, L. A. Electrospinning jets and polymer nanofibers. *Polymer* **49**, 2387–2425 (2008).
30 Yarin, L. A., Kataphinan, W. & Reneker, D. H. Branching in electrospinning of nanofibers. *J. Appl. Phys.* **98**, 064501 (2005).
31 Valiquette, D. & Pellerin, C. Miscible and cores-sheath PS/PVME fibers by electro-spinning. *Macromolecules* **44**, 2838–2843 (2011).
32 Konosu, Y., Matsumoto, H., Tsuboi, K., Minagawa, M. & Tanioka, A. Enhancing the effect of the nanofiber network structure on thermoresponsive wettability switching. *Langmuir* **27**, 14716–14720 (2011).
33 Choi, W., Tuteja, A., Mabry, J. M., Cohen, R. E. & McKinley, G. H. A modified Cassie-Baxter relationship to explain contact angle hysteresis and anisotropy on non-wetting textured surfaces. *J. Colloid Interf. Sci.* **339**, 208–216 (2009).
34 Hardman, S. J., Muhamad-Sarih, N., Riggs, H. J., Thompson, R. L., Rigby, J., Bergius, W. N. A. & Hutchings, L. R. Electrospinning superhydrophobic fibers using surface segregating end-functionalized polymer additives. *Macromolecules* **44**, 6461–6470 (2011).
35 Lim, J. M., Yi, G. R., Moon, J. H., Heo, C. J. & Yang, S. M. Superhydrophobic films of electrospun fibers with multiple-scale surface morphology. *Langmuir* **23**, 7981–7989 (2007).